

# Biotin–Avidin Based Universal Cell–Matrix Interaction for Promoting Three-Dimensional Cell Adhesion

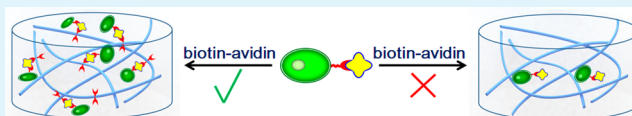
Xiao-Qiu Dou, Jia Zhang, and Chuanliang Feng\*

State Key Lab of Metal Matrix Composites, School of Materials Science and Engineering, Shanghai Jiaotong University, 800 Dongchuan Road, Shanghai, 200240, People's Republic of China

## S Supporting Information

**ABSTRACT:** To promote cell adhesion in three-dimensional (3D) extracellular matrix (ECM) is crucial for avoiding cell anoikis, which is one of the most important issues for fundamental cell biology. Herein, a biotin–avidin based universal cell–matrix interaction for different types of cells is developed in order to achieve the promoted adhesion in 3D ECM. For the purpose, biotinylated nanofibrous hydrogels are constructed by coassembling 1,4-benzylidicarboxamide ( $C_2$ ) based non-biotinylated and biotinylated supramolecular gelators. The used cells are modified by avidin (AV-cells) through biotinylating cells and then interacting with avidin. After in situ encapsulating AV-cells in the hydrogels, the adhered amount can be increased by tens of percent even with adding several percentages of the biotinylated  $C_2$  gelators in the coassembly due to the specific biotin–avidin interaction. Reverse transcription polymerase chain reaction (RT-PCR) confirms that AV-cells can proliferate without varying gene expression and denaturation. Compared with the interaction between RGD and cells, this avidin–biotin interaction should be much more universal and it is feasible to be employed to promote cell adhesion for most types of cells in 3D matrix.

**KEYWORDS:** cell adhesion, biotin–avidin interaction, 3D hydrogel, supramolecular gelator, self-assembly



## INTRODUCTION

To promote cell adhesion in three-dimensional (3D) extracellular matrix (ECM) is crucial for avoiding cell anoikis,<sup>1–4</sup> which is one of the most important issues for fundamental cell biology.<sup>5–7</sup> For encouraging cell adhesion, bioactive molecules (such as RGD<sup>8–12</sup> and growth factors<sup>13–15</sup>) are usually employed. However, bioactive molecules only work for certain target cells and lack universality, leading to cell adhesion greatly dependent on the selected bioactive molecules. In addition, overexpression of genes induced by some growth factors may also have a pathogenic influence on living organisms.<sup>16</sup> To circumvent these limitations, therefore, exploring a universal cell–matrix interaction for most types of cells is becoming an urgent target in order to achieve the enhanced cell adhesion, typically, in 3D matrix.

It is known that almost all kinds of cells have abundant amine groups on their membranes, which can be biotinylated by *N*-hydroxysuccinimide-*D*-biotin (NHS-*D*-biotin).<sup>17–21</sup> Biotinylated cells have been cultured on avidin modified surfaces, and the enhanced cell adhesion is achieved through specific biotin–avidin interaction.<sup>22–25</sup> Biotinylated cells are also cultured into avidin adsorbed polymeric scaffolds and similar phenomena are observed, though their large pores keep them away from 3D biomimetic matrix.<sup>26</sup> Especially the instable physical interaction between avidin and polymers may result in possible dissociation of potential avidin sites used for adhering the biotinylated cells. So far, it is still a big challenge to introduce the biotin–avidin interaction into 3D biomimetic matrix for promoting cell adhesion. To fulfill this, a proper system to construct 3D biomimetic matrix is essential, which should be compatible with

cell survival environments and can be chemically functionalized by avidin or biotin groups. In addition, an in situ cell encapsulation in 3D is also needed. To meet these, supramolecular gelators are one type of potential candidates since they can self-assemble into 3D biomimetic environments.<sup>27–31</sup> Similar to native ECM, their nanofibrous and porous sizes readily respond to the mechanical forces exerted by cells.<sup>32–35</sup> A family of 1,4-benzylidicarboxamide ( $C_2$ ) based supramolecular gelators with the merit of easy functionalization and specific self-assembly properties have been recently reported.<sup>36–38</sup> The well-controlled cell–matrix interaction in the gelators constructed 3D matrix can be obtained after further functionalizing the gelators.<sup>37,38</sup>

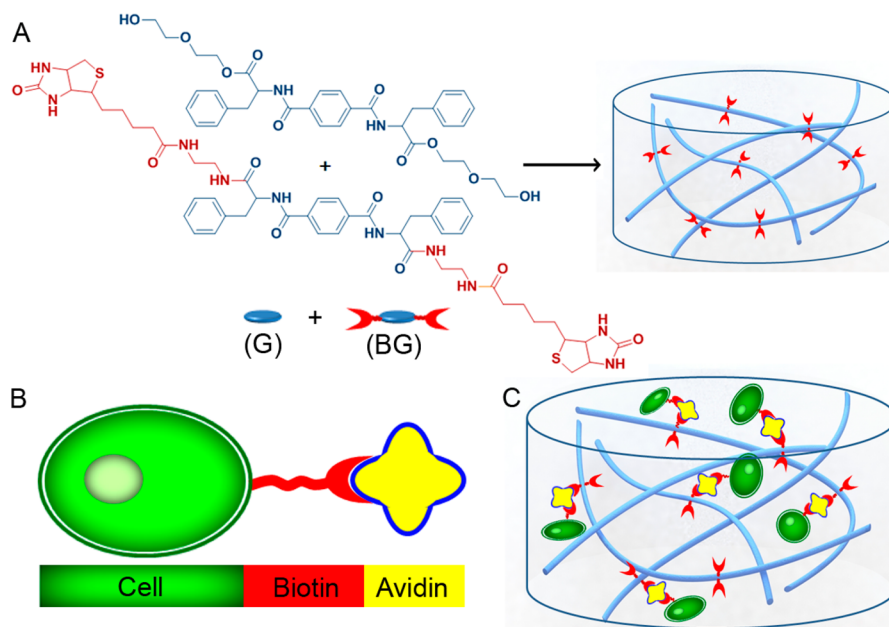
Inspired by the merits of the  $C_2$  based gelators, herein, a biotin–avidin based universal cell–matrix interaction was introduced into 3D supramolecular hydrogels and promoted 3D cell adhesion was successfully achieved. The  $C_2$  gelators were first functionalized by biotin groups in order to achieve biotinylated gelators (BG). By mixing BG and non-biotinylated (G) gelators, they were expected to coassemble into biotinylated 3D nanofibrous hydrogels (Scheme 1A). Being different from previous studies,<sup>22–26</sup> the used cells (MC3T3 osteoblastic, EAhy926 human endothelial, and SMMC-7721 human hepatoma cells) were modified by avidin (AV-cells; Scheme 1B, Schemes S-2 and S-3). After in situ encapsulation into the biotinylated hydrogels, the enhancement of AV-cell

Received: June 29, 2015

Accepted: September 2, 2015

Published: September 2, 2015

**Scheme 1.** (A) (left) Molecular Structures of Non-Biotinylated (G) and Biotinylated Gelators (BG) and (right) Coassembled Biotinylated 3D Networks from G and BG; (B) Schematic Demonstration of Avidin Modified Cell; (C) Enhanced Cell Adhesion in 3D through the Specific Avidin–Biotin Interaction between Avidin Modified Cells and Nanofibers



adhesion may be achieved in 3D matrix because of the specific avidin–biotin interaction (Scheme 1C).

## RESULTS AND DISCUSSION

The C<sub>2</sub> based biotinylated gelator (BG) has the same skeleton as the non-biotinylated gelator (G). Through noncovalent interactions between the skeletons, the biotinylated nanofibers (GBG) could be coassembled by mixing G and BG as characterized by transmission electron microscopy (TEM). Avidin modified Au nanoparticles (Au-avidin) (Figure S-1, diameters ~ 15 nm) were used to determine the coassembled nanofibers (Figure 1A). Au nanoparticles bound to GBG nanofibers were clearly observed (Figure 1B) and further confirmed by energy dispersive spectrometry (EDS) (Figure 1D), suggesting the facile preparation of GBG nanofibers. There were no any Au-avidin particles on the non-biotinylated nanofibers (G), which was ascribed to the lack of the specific biotin–avidin interaction between Au-avidin particles and G nanofibers (Figure 1C).

The GBG hydrogels were made with varying BG mole ratios from 1 to 4 to 6% (Figure S-2), respectively. The interwoven networks of numerous nanofibers were observed for G and all GBG hydrogels (Figure S-3). Information of the nanofibers was collected by circular dichroism (CD) spectra (Figure 2A). All the nanofibers possessed a  $\beta$ -turn structure as characterized by a peak near 218 nm ( $n-\pi^*$  transition) and a trough near 237 nm ( $n-\pi^*$  transition),<sup>39</sup> which confirmed the similarity of molecular arrangement in all the nanofibers. However, the coassembly of G and BG had some effects on spectroscopic and rheological properties of the hydrogels. The introduction of right-handed D-biotin into left-handed helical G nanofibers<sup>38</sup> (Supporting Information) resulted in the decreased intensities of both positive and negative CD peaks due to the racemization.<sup>40</sup> In addition, a negative influence on the storage modulus ( $G'$ ) of the hydrogels with increasing BG percentage was detected by an oscillatory frequency sweep. The  $G'$  was decreased from ~480 to ~385 Pa if 6% BG was incorporated

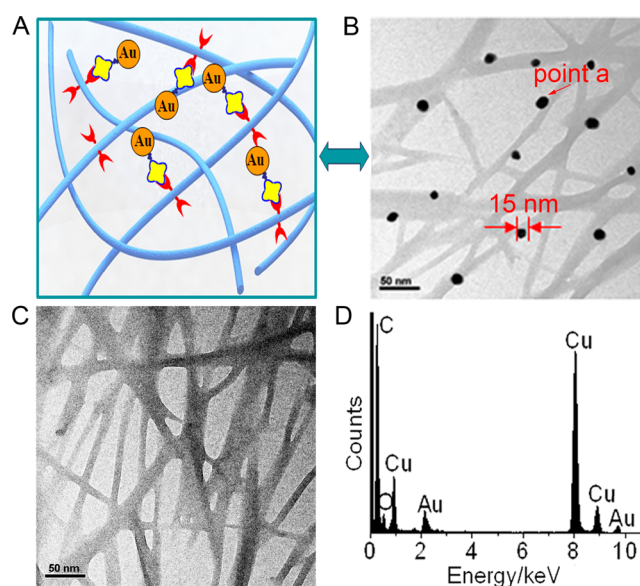


**Figure 1.** (A) Schematic diagram of interaction between Au-avidin nanoparticles and biotinylated nanofibers. (B) TEM image of biotinylated nanofibers (GBG) with attached Au-avidin particles (BG mole percentage 1%). (C) TEM image of non-biotinylated nanofibers (G) without Au-avidin particles. (D) EDS analysis of point a in (B). Cu was from copper grids which were used to support samples. All the scale bars represent 50  $\mu\text{m}$ .

into the hydrogels and the lifetime of GBG hydrogels was also decreased from 21 (0% BG) to 15 days (6% BG). With further increasing BG percentage to 8%, GBG hydrogels were partially disintegrated and degraded into small gel flakes after 11 days.

Before in situ encapsulating cells into GBG hydrogels (Figure S-4), the selected MC3T3 cells were first biotinylated by NHS-D-biotin and then incubated in avidin solution in order to prepare avidin modified MC3T3 cells (AV-MC3T3). The modification was tested by applying Cy3-conjugated biotin

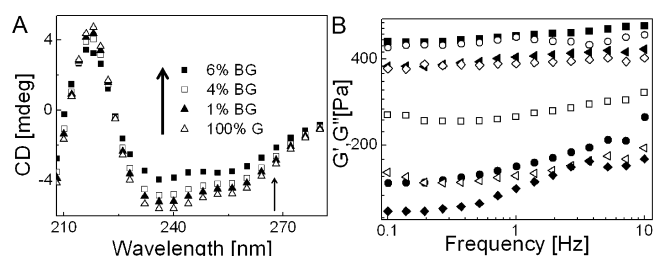


**Figure 2.** (A) CD spectra of diluted G and GBG hydrogel solution. (B) Storage modulus ( $G'$ ) and loss modulus ( $G''$ ) of G and GBG hydrogels as a function of frequency from 0.1 to 10 Hz. (■, □) 100% G; (○, ●) 1% BG; (△, ▽) 4% BG; (◇, ◆) 6% BG; (■, ○, △, ◇)  $G'$ ; (□, ●, ▽, ◆)  $G''$ .

(Cy3-biotin) on the cells. A red fluorescent emission of Cy3 was observed for AV-MC3T3 cells from fluorescent images (Figure 3A), indicating the successful avidin modification for

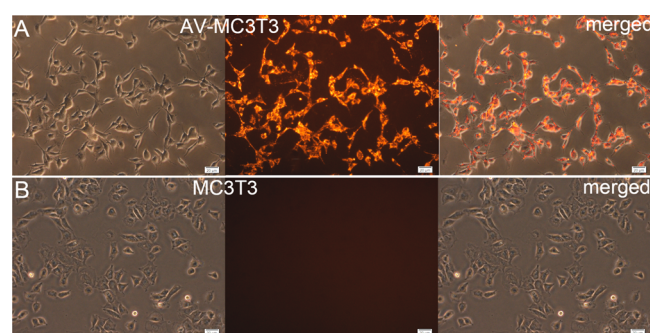


**Figure 3.** Phase contrast and fluorescent images of (A) AV-MC3T3 (with avidin modification) and (B) MC3T3 (without avidin modification) cells after staining by biotin-Cy3. All the scale bars represent 20  $\mu\text{m}$ .

MC3T3 cells, which resulted in avidin–biotin interaction between Cy3-biotin and AV-MC3T3 cells. As expected, there was no red emission for nonavidin modified MC3T3 cells due to lack of the specific avidin–biotin interaction (Figure 3B). Under the conditions of this experiment (see [Avidin Modification of Cells](#)), almost all cells could be modified by avidin as observed from fluorescent images (Figure 3A). The AV-MC3T3 cells were collected by trypsin and then cultured on polystyrene (PS) substrates for 2 h. After applying Cy3-biotin, a red fluorescent emission of Cy3 still existed as observed from fluorescent images (Figure S-5), suggesting that trypsin did not cut off the avidin from the cell surface (if avidin modified on the cell surfaces loses after proteolytic enzyme treatment, the cells should be similar to the ones in the Figure 3B, and not have red fluorescence). Moreover, short-term exposure to the NHS-biotin and avidin solution did not affect cell viability. The viability of AV-MC3T3 on PS surface was proved to be  $\sim 95\%$  (Figure S-6).

AV-MC3T3 cells were encapsulated into GBG hydrogels within one step by mixing them with gelators in culture medium. After 1 day of culture, Live–Dead images showed that AV-MC3T3 preferred to adhere in GBG hydrogels rather than in G ones (Figure 4A). The adhesion densities of AV-MC3T3 (1 day) were increased with incorporating more BG in the hydrogels. Compared with those in G hydrogels, the densities determined by Cell Counting Kit-8 (CCK-8) assays were increased by  $\sim 18$ ,  $\sim 33$ , and  $\sim 48\%$  in GBG hydrogels

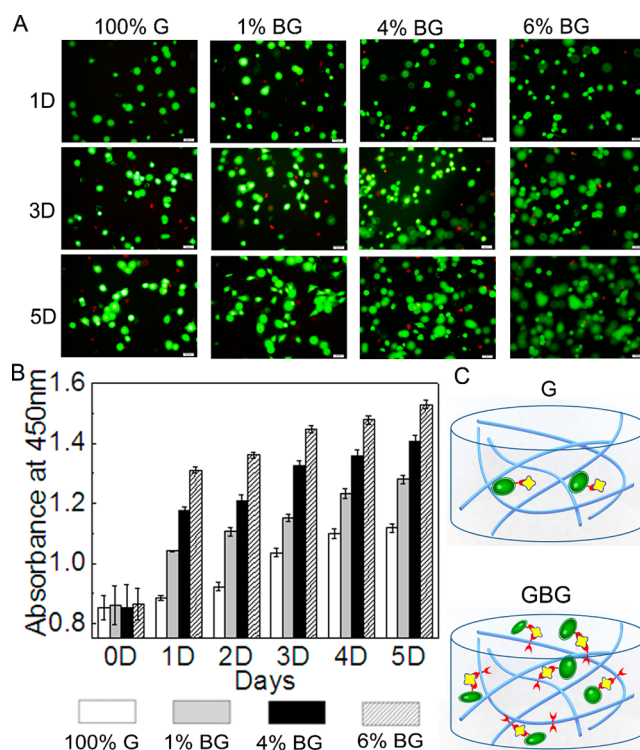


**Figure 4.** (A) Fluorescent images of AV-MC3T3 in G and GBG hydrogels, respectively. Green staining indicates live cells, and red staining indicates dead cells. Scale bars represent 20  $\mu\text{m}$ . (B) CCK-8 measurements of cell viability in G or GBG hydrogels for the indicated days. 0 days means the moment after cell addition in hydrogels. (C) Schematic demonstration of different cell adhesion behaviors in the non-biotinylated (G) and biotinylated (GBG) hydrogels, respectively.

containing 1, 4, and 6% BG, respectively (Figure 4B). Simultaneously, it also led to high cell proliferation densities with prolonging culture time. After 5 days, the corresponding cell densities were enhanced by  $\sim 15$ ,  $\sim 26$ , and  $\sim 37\%$  in 1, 4, and 6% BG containing GBG hydrogels, respectively (Figure 4B). These might be attributed to the existence of the stable avidin sites on GBG nanofibers, ensuring the efficient biotin–avidin interaction between AV-MC3T3 and biotinylated nanofibers (Figure 4C) in the initial culture stage, which resulted in more cell adhesion through communicating with each other and further with nanofibers.<sup>41</sup>

To prove the generality of the approach, avidin modified EAhy926 (AV-EAhy926) and SMMC-7721 tumor (AV-SMMC-7721) cells were cultured in GBG hydrogels (Figure 5). Compared with those in G hydrogels, the adhesion densities (1 day) were increased by  $\sim 36$ ,  $\sim 57$ , and  $\sim 74\%$  for AV-EAhy926 and  $\sim 14$ ,  $\sim 26$ , and  $\sim 33$  for AV-SMMC-7721 with incorporation of 1, 4, and 6% BG in GBG hydrogels, respectively. After 5 days, the high proliferation densities were also achieved in GBG hydrogels for both types of cells. Although of different enhancement ratios for three types of cells due to their respective adhesive properties,<sup>42</sup> e.g., the relatively low increase density of AV-SMMC-7721 might be related to the suspension growth of unattached tumor cells,<sup>43</sup> the adhesion and proliferation in any cases could be greatly enhanced in GBG hydrogels.

The important role of the biotinylated nanofibers in promoting cell adhesion in GBG hydrogels was explored by applying AV-MC3T3 cells on G and GBG nanofibrous films,



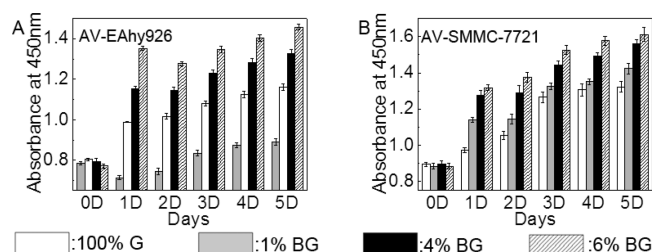


**Figure 5.** CCK-8 assays of viability of avidin modified cells in G or GBG hydrogels for the indicated days. (A) Compared with those in G hydrogels, the adhesion can be respectively increased by  $\sim 38$ ,  $\sim 61$ , and  $\sim 89\%$  for AV-EAhy926 cells in GBG hydrogels containing 1, 4, and 6% BG after 1 day of culture. The corresponding proliferation densities were also respectively increased by  $\sim 31$ ,  $\sim 49$ , and  $\sim 64\%$  compared with those in G hydrogels after 5 days. (B) The adhesion can be respectively increased by  $\sim 17$ ,  $\sim 31$ , and  $\sim 36\%$  for AV-SMMC-7721 cells in GBG hydrogels containing 1, 4, and 6% BG compared with those in G hydrogels after 1 day of culture. The corresponding proliferation densities were also respectively increased by  $\sim 8$ ,  $\sim 18$ , and  $\sim 22\%$  compared with those in G hydrogels after 5 days. 0 days means the moment after cell addition in hydrogels.

respectively. More adhered cells on GBG films were observed than on G films. The increase of cell densities on GBG films could be visualized with prolonging culture time (Figure 6).

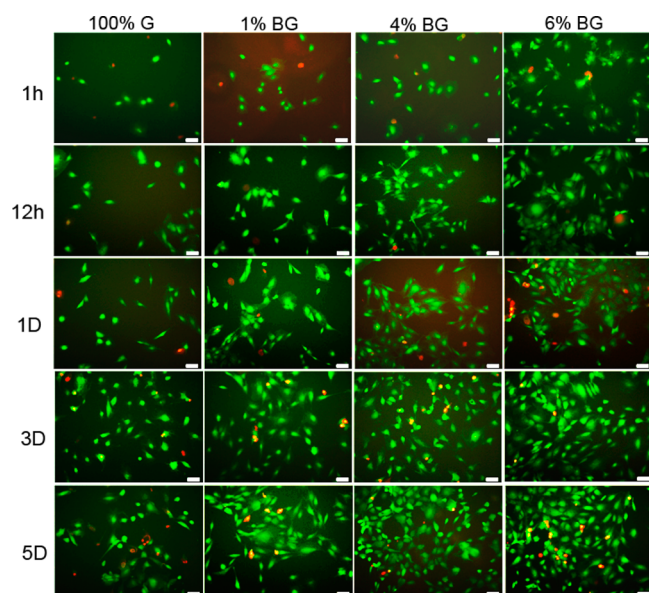


**Figure 6.** AV-MC3T3 cells cultured on G and GBG nanofibrous films after 1 h, 12 h, 1 day, 3 days, and 5 days, respectively. Green staining indicates live cells and red staining indicates dead cells. The more biotin on the films, the more cells adhered on the substrates. Scale bars represent  $50 \mu\text{m}$ .

After 1 day, the measured cell densities by CCK-8 were increased by  $\sim 70$ ,  $\sim 104$ , and  $\sim 128\%$  for AV-MC3T3 on the 1, 4, and 6% BG containing GBG nanofibrous films, respectively (Figure S-7A). The corresponding proliferation densities were enhanced by  $\sim 34$ ,  $\sim 60$ , and  $\sim 89\%$  compared with those on G nanofibrous films after 5 days. Great enhancement for AV-EAhy926 and AV-SMMC-7721 was also achieved on GBG nanofibrous films (Figure S-7B,C). Here, the higher enhancement for the cell adhesion and proliferation densities on GBG nanofibrous films than those in GBG hydrogels may be ascribed

to the more free diffusion of oxygen, nutrients, and metabolites in the culture solution on the nanofibrous films.<sup>44</sup>

The ability of GBG nanofibers to rapidly and selectively enhance cell adhesion was investigated by creating the patterned nanofibrous films by using a microcontact printing method (Figure 7A, Figure S-8).<sup>45</sup> AV-MC3T3 cells were

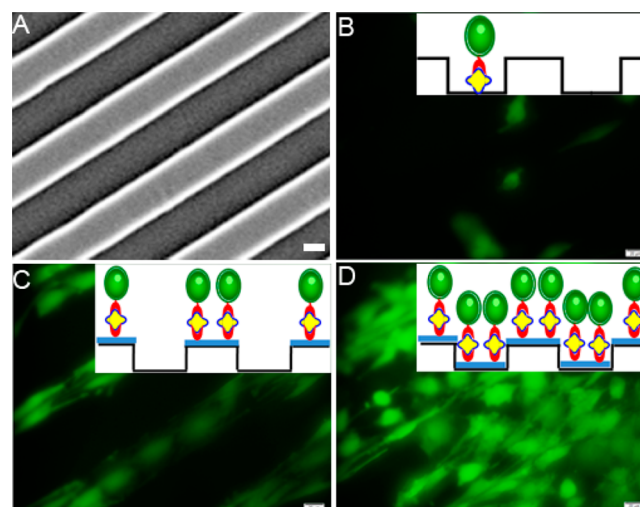


**Figure 7.** (A) Scanning electron microscopic (SEM) image of the patterned PS surface. (B) Fluorescent image of AV-MC3T3 cells on patterned PS films. (C) Fluorescent image of AV-MC3T3 on patterned films with the top strip coated by GBG nanofibers. (D) Fluorescent image of AV-MC3T3 on patterned films with both the top strip and grooves coated by GBG nanofibers. Scale bars represent  $20 \mu\text{m}$ .

seeded on all patterned films and fresh Dulbecco's modified Eagle's medium (DMEM) was used to remove nonadhered cells after 15 min. Only several cells were observed on the patterned PS films in fluorescent images after 1 day (Figure 7B). However, if AV-MC3T3 cells were cultured on the patterns with GBG nanofibers coated on the top strips, many more cells selectively proliferated along the strips and with the elongated morphologies (Figure 7C). If both the top strips and grooves were coated by GBG nanofibers, the elongated AV-MC3T3 proliferated not only on the top strips, but also in the grooves (Figure 7D). The results implied that the biotin–avidin interaction could rapidly and selectively promote cell adhesion through the specific interaction between AV-MC3T3 and GBG nanofibers, which simultaneously encouraged cell proliferation on GBG nanofibers.

Verification of the necessity to modify cells by avidin for encouraging cell adhesion in GBG hydrogels was followed. Unmodified MC3T3, EAhy926, and SMMC-7721 cells were encapsulated in GBG and G hydrogels, respectively. After 1 day, the cell densities by CCK-8 were only increased by less than 10% for three different cells in GBG hydrogels containing 1, 4, and 6% BG compared with those in G hydrogels (Figures S-9 and S-10). The proliferation densities in GBG hydrogels were also similar to those in G hydrogels within culture days. These should be attributed to the absence of the specific avidin–biotin interaction between the cells and GBG hydrogels. Here, the biotin molecule itself could slightly promote cell adhesion in GBG gels.<sup>46</sup>

The possible influence on gene expression of avidin modified cells was tested by reverse transcription polymerase chain

reaction (RT-PCR). Four representative genes of MC3T3 cells (alkaline phosphatase, RunX2, osteonectin, and osteopontin) were analyzed in three different groups (group A, MC3T3 cells cultured on PS; group B, AV-MC3T3 cells on PS; group C, AV-MC3T3 cells on GBG fibers). There was not much difference in the expression level of these genes in three groups (Figure S-11), which proved that the cell treatment by biotinylation and avidin modification would not alter normal gene expression; however, it usually occurred with growth factors.<sup>16</sup>

The effectiveness of the method to promote cell adhesion and proliferation in 3D was further judged by using RGD functionalized G hydrogels as control (Supporting Information). The unmodified 7721 cells were encapsulated into the RGD functionalized hydrogels (6% RGD) within one step. After 5 days, similar amounts of live cells in GBG hydrogels and RGD functionalized hydrogels were obtained, respectively (Figure S-12), implying that the approach can play a similar role as RGD during promoting cell adhesion and proliferation in 3D hydrogels.

## CONCLUSION

By using the biotinylated C<sub>2</sub> gelators and avidin modified cells, a biotin–avidin based universal cell–matrix interaction is introduced into 3D matrix, which may selectively and rapidly promote cell adhesion in 3D and in turn induce high proliferation densities. The densities can be increased by tens of percent even with several percentages of the biotinylated C<sub>2</sub> gelators in the coassembly. The study may circumvent the limitation from bioactive molecules for encouraging cell adhesion in matrix, which is typically beneficial to the cells with the difficultly obtained bioactive molecules and the cells that are difficult to adhere on biomaterials (e.g., nerve cells).<sup>47</sup> Because of the feasibility to modify different types of cells by avidin, this biotin–avidin based interaction should be not a unique but a common drive to promote cell adhesion and proliferation for most types of cells in 3D. Thus, the study not only develops a universal methodology for encouraging cell culture in 3D matrix, but also paves a new way to functionalize 3D matrix for avoiding cell anoikis during cell culture, which may find broad applications in the field of tissue engineering, e.g., tissue repair.<sup>48</sup>

## EXPERIMENTAL SECTION

**Synthesis of Gelator (G), Biotinylated Gelator (BG), and RGD Modified Gelator (RG).** L-Phenylalanine methyl ester hydrochloride, 1,4-benzenedicarbonyl dichloride, and diglycol were purchased from Aladdin Chemicals and used without further purification. The detailed synthesis of gelator G is in ref 37. <sup>1</sup>H NMR experiments were performed by using a Bruker Advance III 400 instrument operated at 400 MHz. Mass spectra were recorded on a Waters Q-ToF Premier mass spectrometer by positive mode electrospray ionization.

To synthesize gelators BG and RG (Scheme S-1), intermediate compound G0 (Scheme S-1) was first prepared in our lab through the liquid phase reaction between L-phenylalanine methyl ester hydrochloride and 1,4-benzenedicarbonyl dichloride. The detailed synthesis of intermediate compound G0 is in ref 37. G0 was provided to Chinapeptides Co. (Shanghai) to further synthesize gelators BG and RG through solid phase synthesis. The purities of BG and RG were both >95%.

**Materials and Characterization.** Au-avidin particles were purchased from Shanghai Anyan Trading Co. CD spectra were collected by a JASCO J-815 CD spectrometer with a bandwidth of 1.0 nm. TEM samples were placed on copper grids to be observed. TEM images were obtained with a transmission electron microscope (JEM-2010). SEM samples were placed on silicon slices to be observed. SEM

samples were visualized with an FEI QUANTA 250. The rheology was measured with a TA Instruments AR G2 rheometer.

**Avidin Modification of Cells.** Cells were biotinylated with the commercially available reagent N-hydroxysuccinimide-D-biotin (NHS-D-biotin, Scheme S-2). Cells were first cultured on plates for 4 h, and phosphate-buffered saline (PBS) was used to wash the nonadhered cells. NHS-D-biotin (5 μg/mL) aqueous solution was refilled on the plate. The plates were then incubated in a CO<sub>2</sub> incubator (37 °C) for 10 min and in a refrigerator (4 °C) for 30 min. After removing NHS-D-biotin, the biotinylated cells were washed with PBS again and recovered with avidin aqueous solution (2 mg/mL) for 10 min to form biotin–avidin complexes on the cell surface (Scheme S-3). The avidinylated rate of cells was tested by using Cy3-biotin (Littlepasciences, China). The Cy3-biotin solution (2.5 mg/mL in DMEM without fetal bovine serum) was used to treat the cells for 2 h in the incubator (37 °C, 5% CO<sub>2</sub>). After washing with PBS, the cells were viewed under a fluorescence microscope with excitation filters of 494 nm. The avidinylated rate of cells was counted at least 10 visual fields within a 100× field.

**3D and 2D Cell Culture.** The MC3T3, EAhy926, and SMMC-7721 cells were provided by Prof. Guangyin Yuan (School of Materials Science and Engineering, Shanghai Jiaotong University). For 3D cell culture, 20 μL of the gelators (BG or G) in DMSO solution (300 mg/mL) was transferred into a test tube, and mixed with 980 μL of cell suspension (1 × 10<sup>6</sup> cells). A 100 μL volume of the above cell suspension was then added into the well (96 well plates) and incubated for 2 min under a humidified atmosphere of 5% CO<sub>2</sub> at 37 °C for gelation. Another 100 μL of DMEM was then added on the top of the gel. For 2D cell culture, 100 μL of gelators (0.1 mg/mL) was added into one well of 96 well plates. The plates were dried in a vacuum oven under 37 °C, and the G or GBG films formed on the surface of plates. A 100 μL volume of cell suspension (5 × 10<sup>4</sup> cells) was added into one well of a 96 well plate coated with dried films.

**Live–Dead Staining Assay and CCK-8.** A fluorescent Live–Dead staining assay was used to visualize the proportion of viable and nonviable cells after 24 h. A Cell Counting Kit-8 (CCK-8) was employed to quantitatively evaluate cell viability. A 10 μL volume of the CCK-8 solution was added into each well of the 96 well plate. The plates were then incubated for 2 h in the incubator before measurement of the absorbance at 450 nm.

**Reverse Transcription PCR.** Total RNA from MC3T3 cells was isolated by using TRIZOL (Invitrogen) following the manufacturer's protocol. Aliquots of the RT products were used for semiquantitative RT-PCR analysis. PCR products were visualized by electrophoresis on a 2% agarose gel in 0.5× Tris–borate–EDTA (TBE) buffer after staining with 0.5 μg/mL ethidium bromide.

## ASSOCIATED CONTENT

### Supporting Information

The Supporting Information is available free of charge on the ACS Publications website at DOI: 10.1021/acsami.5b05828.

Synthetic routes of gelators G and BG; morphological study; modification of cells; reverse transcription PCR; cell test (PDF)

## AUTHOR INFORMATION

### Corresponding Author

\*E-mail: clfeng@sjtu.edu.cn.

### Notes

The authors declare no competing financial interest.

## ACKNOWLEDGMENTS

We thank the National Science Foundation of China (51273111,51173105), the National Basic Research Program of China (973 Program 2012CB933803), and the Program for



Professors of Special Appointment (Eastern Scholar) at Shanghai Institutions of Higher Learning, SRF for ROCS, SEM.

## ■ REFERENCES

- (1) Sun, T. L.; Han, D.; Rhemann, K.; Chi, L. F.; Fuchs, H. Stereospecific Interaction between Immune Cells and Chiral Surfaces. *J. Am. Chem. Soc.* **2007**, *129*, 1496–1497.
- (2) Sun, T. L.; Qing, G. Y.; Su, L. B.; Jiang, L. Functional Biointerface Materials Inspired from Nature. *Chem. Soc. Rev.* **2011**, *40*, 2909–2921.
- (3) Wang, X.; Gan, H.; Zhang, M. X.; Sun, T. L. Modulating Cell Behaviors on Chiral Polymer Brush Films with Different Hydrophobic Side Groups. *Langmuir* **2012**, *28*, 2791–2798.
- (4) Wang, X.; Gan, H.; Sun, T. L.; Su, B. L.; Fuchs, H.; Vestweber, D.; Butz, S. Stereochemistry Triggered Differential Cell Behaviours on Chiral Polymer Surfaces. *Soft Matter* **2010**, *6*, 3851–3855.
- (5) Liu, X. L.; Wang, S. T. Three-Dimensional Nano-Biointerface as a New Platform for Guiding Cell Fate. *Chem. Soc. Rev.* **2014**, *43*, 2385–2401.
- (6) Meng, J. X.; Liu, H. L.; Liu, X. L.; Yang, G.; Zhang, P. C.; Wang, S. T.; Jiang, L. Hierarchical Biointerfaces Assembled by Leukocyte-Inspired Particles for Specifically Recognizing Cancer Cells. *Small* **2014**, *10*, 3735–3741.
- (7) Jin, J.; Xing, Y. Z.; Xi, Y. L.; Liu, X. L.; Zhou, T.; Ma, X. X.; Yang, Z. Q.; Wang, S. T.; Liu, D. S. A Triggered DNA Hydrogel Cover To Envelop and Release Single Cells. *Adv. Mater.* **2013**, *25*, 4714–4717.
- (8) Boekhoven, J.; Rupert Pérez, C. M.; Sur, S.; Worthy, A.; Stupp, S. I. Dynamic Display of Bioactivity through Host-Guest Chemistry. *Angew. Chem., Int. Ed.* **2013**, *52*, 12077–12080.
- (9) Berns, E. J.; Sur, S.; Pan, L. L.; Goldberger, J. E.; Suresh, S.; Zhang, S. M.; Kessler, J. A.; Stupp, S. I. Aligned Neurite Outgrowth and Direct Cell Migration in Self-Assembled Monodomain Gels. *Biomaterials* **2014**, *35*, 185–195.
- (10) Liu, D. B.; Xie, Y. Y.; Shao, H. W.; Jiang, X. Y. Using Azobenzene-Embedded Self-Assembled Monolayers To Photochemically Control Cell Adhesion Reversibly. *Angew. Chem., Int. Ed.* **2009**, *48*, 4406–4408.
- (11) Cao, B.; Peng, R.; Li, Z. H.; Ding, J. D. Effects of Spreading Areas and Aspects Ratios of Single Cells on Dedifferentiation of Chondrocytes. *Biomaterials* **2014**, *35*, 6871–6881.
- (12) Zhang, Z.; Lai, Y. X.; Yu, L.; Ding, J. D. Effects of Immobilizing Sites of RGD Peptides in Amphiphilic Block Copolymers on Efficacy of Cell Adhesion. *Biomaterials* **2010**, *31*, 7873–7882.
- (13) Davis, M. E.; Hsieh, P. C. H.; Takahashi, T.; Song, Q.; Zhang, S. G.; Kamm, R. D.; Grodzinsky, A. J.; Anversa, P.; Lee, R. T. Local Myocardial Insulin-Like Growth Factor 1 (IGF-1) Delivery with Biotinylated Peptide Nanofibers Improves Cell Therapy for Myocardial Infarction. *Proc. Natl. Acad. Sci. U. S. A.* **2006**, *103*, 8155–8160.
- (14) Wu, E. C.; Zhang, S. G.; Hauser, C. A. E. Self-Assembling Peptides as Cell-Interactive Scaffolds. *Adv. Funct. Mater.* **2012**, *22*, 456–468.
- (15) Liu, X.; Wang, X. M.; Horii, A.; Wang, X. J.; Qiao, L.; Zhang, S. G.; Cui, F. Z. In Vivo Studies on Angiogenic Activity of Two Designer Self-Assembling Peptide Scaffold Hydrogel in the Chicken Embryo Chorioallantoic Membrane. *Nanoscale* **2012**, *4*, 2720–2727.
- (16) Richmond, A. The Pathogenic Role of Growth-Factors in Melanoma. *Semin. Dermatol.* **1991**, *10*, 246–255.
- (17) Tsai, W. B.; Wang, M. C. Effect of an Avidin-Biotin Binding System on Chondrocyte Adhesion, Growth, and Gene Expression. *Biomaterials* **2005**, *26*, 3141–3151.
- (18) Tsai, W. B.; Wang, M. C. Effect of an Avidin-Biotin Binding System on Chondrocyte Adhesion and Growth on Biodegradable Polymers. *Macromol. Biosci.* **2005**, *5*, 214–221.
- (19) Tsai, W. B.; Wang, P. Y.; Chang, Y.; Wang, M. C. Fibronectin and Culture Temperature Modulate the Efficacy of an Avidin-Biotin Binding System for Chondrocyte Adhesion and Growth on Biodegradable Polymers. *Biotechnol. Bioeng.* **2007**, *98*, 498–507.
- (20) Krishnamachari, Y.; Pearce, M. E.; Salem, A. K. Self-Assembly of Cell-Microparticle Hybrids. *Adv. Mater.* **2008**, *20*, 989–993.
- (21) Wang, B.; Song, J. Z.; Yuan, H. X.; Nie, C. Y.; Lv, F. T.; Liu, L. B.; Wang, S. Multicellular Assembly and Light-Regulation of Cell-Cell Communication by Conjugated Polymer Materials. *Adv. Mater.* **2014**, *26*, 2371–2375.
- (22) Chan, B. P.; Reichert, W. M.; Truskey, G. A. Effect of Streptavidin-Biotin on Endothelial Vasoregulation and Leukocyte Adhesion. *Biomaterials* **2004**, *25*, 3951–3961.
- (23) Mathur, A. B.; Chan, B. P.; Truskey, G. A.; Reichert, W. M. High-Affinity Augmentation of Endothelial Cell Attachment: Long-Term Effects on Focal Contact and Actin Filament Formation. *J. Biomed. Mater. Res.* **2003**, *66A*, 729–737.
- (24) Bhat, V. D.; Truskey, G. A.; Reichert, W. M. Using Avidin-Mediated Binding to Enhance Initial Endothelial Cell Attachment and Spreading. *J. Biomed. Mater. Res.* **1998**, *40*, 57–65.
- (25) Gong, P. Y.; Zheng, W. F.; Huang, Z.; Zhang, W.; Xiao, D.; Jiang, X. Y. A Strategy for the Construction of Controlled, Three-Dimensional, Multilayered, Tissue-Like Structures. *Adv. Funct. Mater.* **2013**, *23*, 42–46.
- (26) Kojima, N.; Matsuo, T.; Sakai, Y. Rapid Hepatic Cell Attachment onto Biodegradable Polymer Surfaces without Toxicity Using an Avidin-Biotin Binding System. *Biomaterials* **2006**, *27*, 4904–4910.
- (27) Kloxin, A. M.; Kasko, A. M.; Salinas, C. N.; Anseth, K. S. Photodegradable Hydrogel for Dynamic Tuning of Physical and Chemical Properties. *Science* **2009**, *324*, 59–63.
- (28) Luo, Z. L.; Zhang, S. G. Designer Nanomaterials Using Chiral Self-Assembling Peptide Systems and Their Emerging Benefit for Society. *Chem. Soc. Rev.* **2012**, *41*, 4736–4754.
- (29) Boekhoven, J.; Stupp, S. I. 25th Anniversary Article: Supramolecular Materials for Regenerative Medicine. *Adv. Mater.* **2014**, *26*, 1642–1659.
- (30) Miao, X. M.; Cao, W.; Zheng, W. T.; Wang, J. Y.; Zhang, X. L.; Gao, J.; Yang, C. B.; Kong, D. L.; Xu, H. P.; Wang, L.; Yang, Z. M. Switchable Catalytic Activity: Selenium-Containing Peptides with Redox-Controllable Self-Assembly Properties. *Angew. Chem., Int. Ed.* **2013**, *52*, 7781–7785.
- (31) Shi, Y.; Wang, J. Y.; Wang, H. M.; Hu, Y. H.; Chen, X. M.; Yang, Z. M. Glutathione-Triggered Formation of a Fmoc-Protected Short Peptide-Based Supramolecular Hydrogel. *PLoS One* **2014**, *9*, e106968.
- (32) Capito, R. M.; Azevedo, H. S.; Velichko, Y. S.; Mata, A.; Stupp, S. I. Self-Assembly of Large and Small Molecules into Hierarchically Ordered Sacs and Membranes. *Science* **2008**, *319*, 1812–1816.
- (33) Barnard, A.; Posocco, P.; Priel, S.; Calderon, M.; Haag, R.; Hwang, M. E.; Shum, V. W. T.; Pack, D. W.; Smith, D. K. Degradable Self-Assembling Dendrons for Gene Delivery: Experimental and Theoretical Insights into the Barriers to Cellular Uptake. *J. Am. Chem. Soc.* **2011**, *133*, 20288–20300.
- (34) Bromfield, S. M.; Wilde, E.; Smith, D. K. Heparin Sensing and Binding-Taking Supramolecular Chemistry towards Clinical Applications. *Chem. Soc. Rev.* **2013**, *42*, 9184–9195.
- (35) Cornwell, D. J.; Okesola, B. O.; Smith, D. K. Hybrid Polymer and Low Molecular Weight Gels-Dynamic Two-Component Soft Materials with Both Responsive and Robust Nanoscale Networks. *Soft Matter* **2013**, *9*, 8730–8736.
- (36) Feng, C. L.; Dou, X. Q.; Zhang, D.; Schoenherr, H. A Highly Efficient Self-Assembly of Responsive C<sub>2</sub>-Cyclohexane-Derived Gelators. *Macromol. Rapid Commun.* **2012**, *33*, 1535–1541.
- (37) Dou, X. Q.; Li, P.; Zhang, D.; Feng, C. L. RGD Anchored C<sub>2</sub>-Benzene Based PEG-Like Hydrogels as Scaffolds for Two and Three Dimensional Cell Cultures. *J. Mater. Chem. B* **2013**, *1*, 3562–3568.
- (38) Liu, G. F.; Zhang, D.; Feng, C. L. Control of Three-Dimensional Cell Adhesion by the Chirality of Nanofibers in Hydrogels. *Angew. Chem., Int. Ed.* **2014**, *53*, 7789–7793.
- (39) Ma, M.; Kuang, Y.; Gao, Y.; Zhang, Y.; Gao, P.; Xu, B. Aromatic-Aromatic Interactions Induce the Self-Assembly of Pentapeptidic Derivatives in Water To Form Nanofibers and Supramolecular Hydrogels. *J. Am. Chem. Soc.* **2010**, *132*, 2719–2728.

(40) Lee, C. C.; Grenier, C.; Meijer, E. W.; Schenning, A. P. H. J. Preparation and Characterization of Helical Self-Assembled Nanofibers. *Chem. Soc. Rev.* **2009**, *38*, 671–683.

(41) Nuttelman, C. R.; Mortisen, D. J.; Henry, S. M.; Anseth, K. S. Attachment of Fibronectin to Poly(Vinyl Alcohol) Hydrogels Promotes NIH3T3 Cell Adhesion, Proliferation, and Migration. *J. Biomed. Mater. Res.* **2001**, *57*, 217–223.

(42) Cheresh, D. A.; Smith, J. W.; Cooper, H. M.; Quaranta, V. A. Novel Vitronectin Receptor Integrin (Alpha-V-Beta-X) is Responsible for Distinct Adhesive Properties of Carcinoma-Cells. *Cell* **1989**, *57*, 59–69.

(43) Wang, Y.; Liu, Y. H.; Jiang, J. S.; Cui, H. B. Inhibitory Effect of Matrine on Proliferation, Invasion and Metastasis of Hepatocellular Carcinoma Stem Cells. *Chin. J. Exp. Surg.* **2013**, *1*, 61–63.

(44) Cukierman, E.; Pankov, R.; Stevens, D. R.; Yamada, K. M. Taking Cell-Matrix Adhesions to the Third Dimension. *Science* **2001**, *294*, 1708–1712.

(45) Feng, C. L.; Embrechts, A.; Bredebusch, I.; Schnekenburger, J.; Domschke, W.; Vancso, G. J.; Schonherr, H. Reactive Microcontact Printing on Block Copolymer Films: Exploiting Chemistry in Microcontacts for Sub-Micrometer Patterning of Biomolecules. *Adv. Mater.* **2007**, *19*, 286–290.

(46) Crisp, S. E. R. H.; Griffin, J. B.; White, B. R.; Toombs, C. F.; Camporeale, C.; Said, H. M.; Zemleni, J. Biotin Supply Affects Rates of Cell Proliferation, Biotinylation of Carboxylases and Histones, and Expression of the Gene Encoding the Sodium-Dependent Multivitamin Transporter in Jar Choriocarcinoma Cells. *Eur. J. Nutr.* **2004**, *43*, 23–31.

(47) Schubert, D.; Whitlock, C. Alteration of Cellular Adhesion by Nerve Growth Factor. *Proc. Natl. Acad. Sci. U. S. A.* **1977**, *74*, 4055–4058.

(48) Kang, A.; Park, J.; Ju, J.; Jeong, G. S.; Lee, S. H. Cell Encapsulation via Microtechnologies. *Biomaterials* **2014**, *35*, 2651–2663.